Table 1. Calibration of pipettes by the fluorometric and radioisotope techniques (S.D., standard deviation).

Pipette No.	Diameter (μ) and length (mm) of quartz tubing	No. of deliveries	Volume (nl)	S.D. (nl)
	Fluorometric technique			
1	43(1.0)	9	1.86	0.03
2	43(1.4)	8	2.51	.02
3	43(2.0)	9	3.90	.04
4	90(1.25)	9	8.50	.09
	Radioisotope technique			
5	43(15.4)	3	103.2	2.55
6	90(30.7)	3	189.8	0.88

Table 2. Comparison of methods used for pipetting during calibration by fluorometry.

Pipette No.	No. of deliveries	Volume (nl)	S.D. (nl)
	Rinsed with diluent		
2	9	2.51	0.02
3	9	3.90	.04
	Complete delivery; no rinse		
2		2.43	0.03
3		3.87	.03
	Incomplete delivery; no rinse		
2		2.41	0.04
3		3.83	.06

short distance and used to heat the quartz until it can be drawn and completely separated. The pipette, with this extra quartz, is manipulated over to a brass block beneath the cutter, where it is carefully positioned so that the cutter removes the extra tubing. The cutter is a sharpened silicon-carbide chip, silver-soldered to a handle which is hinge-mounted on the aluminum block.

The pipettes may be calibrated either by fluorometric or radioisotope techniques. For fluorometric calibration, a stock solution of quinine in 0.1*N* sulfuric acid is made, and accurate standards are obtained by diluting the stock solution in distilled water to give dilutions of $1 : 10^6$ to $10 : 10^6$. Readings of these standards are taken on an Aminco-Bowman spectrophotofluorometer and a standard curve is drawn. Then the nanoliter pipettes are calibrated by pipetting from the stock quinine solution into 1 ml of distilled water and comparing these readings with the standard curve. To check reproducibility, the procedure is repeated a number of times for each pipette and the mean volume and standard deviation computed from the readings. Table 1 shows the results obtained from six of our pipettes selected at random. The first four pipettes were calibrated by the method just described; numbers 5 and 6 were calibrated by a radioisotope technique in which Na^{22} was used.

With each of the four pipettes calibrated by fluorescence, stock solution was transferred into the 1 ml of distilled water and the pipette subsequently rinsed with the solution. To prevent blowing air bubbles, the pipette was not completely emptied of the stock solution, but the amount remaining was rinsed out several times. Table 2 shows a comparison between this method of pipetting and two other methods. In the second method, the entire volume of stock solution was emptied until an air bubble was formed; the pipette was not rinsed with the solution. The apparent volume was slightly less, but the reproducibility was as good or better than with rinsing. The third method depended on incomplete delivery—that is, delivery of all the contents of the pipette except for a very small amount in the tip. No bubbles were blown, and the pipette was not rinsed with the solution. As expected, the apparent volume was less than that of either of the other two methods and the standard deviation was not as small. The amount to which this effect is noticeable depends on the length and diameter of the tip of the pipette.

As with all pipettings performed with nanoliter volumes, it is essential that the deliveries be made under microscopic observation. It is preferable that both ends of the quartz be in the field of vision so that filling and emptying can be observed. To reduce the length of the quartz required for pipettes of larger volume, it is a simple matter to form a bulb in the quartz outside the seal by heating a point with the microflame and applying pressure with the syringe.

The pipettes described can be made for volumes ranging from fractions of nanoliters to hundreds of nanoliters with reproducibilities of 1 percent over the entire range. In addition, the approximate volume of the pipettes can be quickly calculated and accurate calibration is relatively simple with the fluorescence technique outlined. Construction is simple, and with practice, as many as six to ten can be made per hour by our rather crude system. With the increased research into the minutiae of biological organisms and the resultant increase in the use of microchemical techniques these pipettes should find use in many laboratories.

DENIS J. PRAGER
ROBERT L. BOWMAN
GERALD G. VUREK
Laboratory of Technical Development, National Heart Institute, Bethesda, Maryland 20014

Notes

1. Flint glass capillary tubing nominally 1.0 mm outside diameter and 100 mm long; catalog No. V48302, Aloe Scientific Company.
2. Santotube "Q" quartz tubing, Monsanto Research Corporation, Nicholas Road, Dayton, Ohio.

15 December 1964

Late-Wisconsin End Moraines in Northern Canada

Abstract. *A system of end moraines nearly 2240 kilometers long has been identified by field investigation and aerial photography. It extends through northeastern Keewatin, Melville Peninsula, and Baffin Island and marks the border of a late-Wisconsin ice sheet centered over Foxe Basin and Hudson Bay 8000 or 9000 years ago.*

The late-Wisconsin glacial history of northern Canada remained largely conjectural until recently. The broad distribution of glacial features, mainly formed during deglaciation, were shown on the Glacial Map of Canada (*1*). The information on which this map is based varies considerably in reliability, with the result that large areas of the Canadian Arctic, notably Baffin Island, Melville Peninsula, and northeast Labrador-Ungava, are misleadingly shown to lack glacial features.

Our field investigations and interpretation of aerial photographs, together with study of the literature (*2–5*), show the existence of a major end-moraine system traceable, with relatively few gaps, for over 2240 km along the east coast of Baffin Island, on the west coast of Melville Peninsula, and westward across Keewatin between Committee Bay and Chantrey Inlet, with an increasing southwesterly trend to within 110 km of the head of Bathurst Inlet; thence it turns southward to Back River, beyond which it becomes indistinct (Fig. 1). An extensive system of end and lateral moraines in northeast Labrador-Ungava may be re-

lated to it. We believe that the outline of the moraine system delineates the northern and eastern borders of a late-Wisconsin ice sheet.

Field investigations by Ives and Andrews (*4*) revealed widespread and complex development of the end-moraine system on eastern Baffin Island; they tentatively distinguished two broad phases—Cockburn I and II—represented by the outer and inner portions of the moraine belt. Sim (*5*) reported a large kame moraine on the west coast of Melville Peninsula and postulated an ice body in Committee Bay to account for its formation. On the basis of aerial-photograph mapping of glacial features, however, we believe that the Melville Peninsula moraine marked the western boundary of an ice sheet centered over Foxe Basin, and that it is the equivalent of part of the Cockburn moraine belt on Baffin Island. Prominent moraines north of Fury and Hecla Strait and in the Bernier Bay area of Baffin Island have been mapped and may be further links with the Cockburn system. On northern Baffin Island we have obtained radiocarbon dates from the marine mollusc shells found in association with Cockburn terminal moraines in Milne Inlet and Tay Sound which suggest minimum ages of 7930 ± 300 (I-1246) and 8350 ± 300 years (I-724), respectively, for the terminal moraines (Fig. 1).

When the importance and extent of the Cockburn moraine system was realized, interpretation of aerial photographs of the northern Keewatin mainland was repeated, confirming the existence of a moraine system first mapped from air photographs in 1955 (*6*). In Craig's more recent works on the Keewatin sector (*7*) he mapped the approximate limit of marine submergence in the Chantrey Inlet area and suggested that the sea reached its maximum stand here at least 8870 ± 140 years ago (GSC-44). When Craig's marine limit is superimposed upon our map of the moraine system, parts of the two features coincide, implying a minimum age of 8870 years for this section of end moraine. West of the immediate vicinity of Chantrey Inlet the moraine mainly takes the form of a single massive ridge, much of which has been traced independently by Blake (*2*); shells of marine molluscs (collected by Blake in the MacAlpine Lake area) which are thought to have lived concurrently with deposition of the moraine have been dated 8160 ± 140 years (GSC-110).

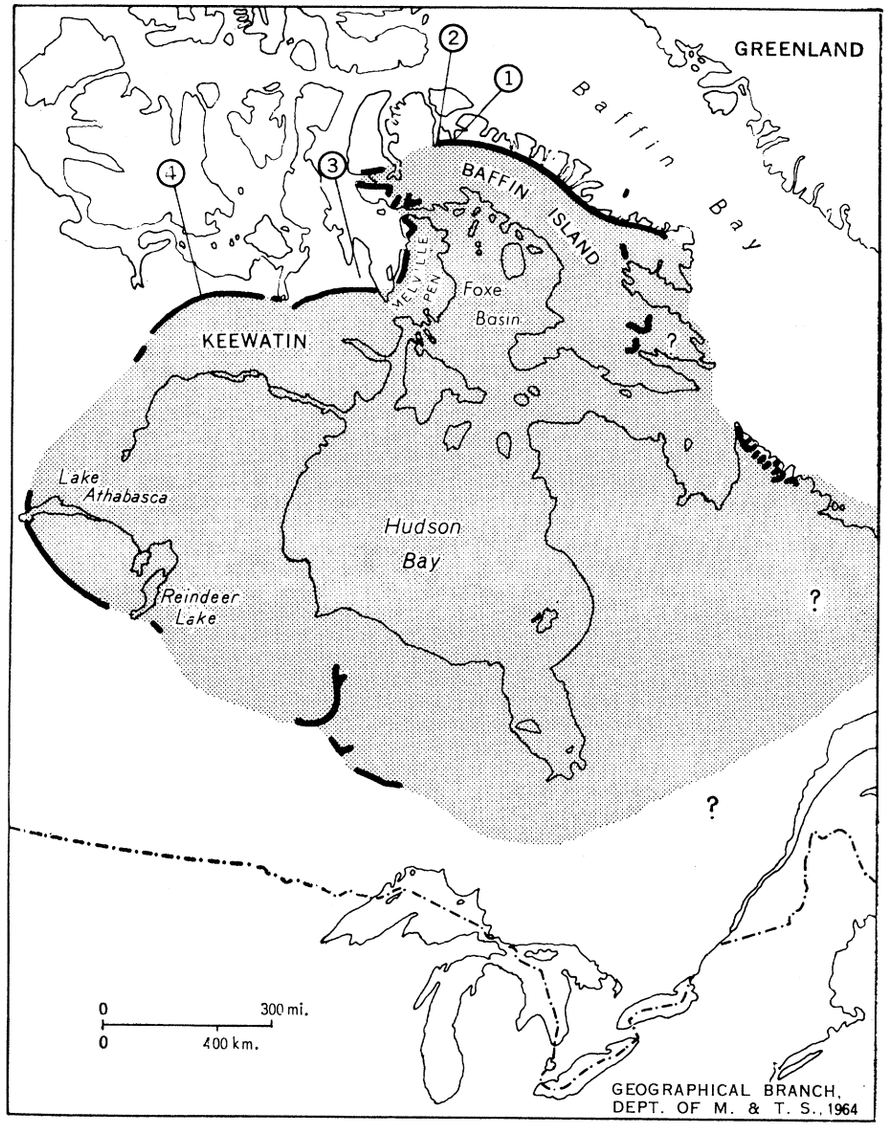

Fig. 1. Area covered by postulated late-Wisconsin ice sheet is shown by gray tone. Generalized positions of known end moraines and moraine belts are shown by thick lines. Sources of samples dated by radiocarbon: *1*, Tay Sound; *2*, Koluktoo Bay; *3*, sample used to infer date of Chantrey Inlet moraine; *4*, MacAlpine Lake.

The spatial near-continuity of the system and the reasonable agreement of the estimated ages of its various sections suggest that the end-moraine system outlines a large continental ice sheet centered over Foxe Basin and Hudson Bay between 8000 and 9500 years ago. The Cockburn moraines of eastern Baffin Island are much more complex; we believe that their formation spans a much longer period ranging from 5000 to more than 10,000 years ago. This complication, however, does not detract from the contention that, when the various sections of moraine are plotted on a small scale map, the plot represents the outline of an ice sheet as it existed some 8000 or 9000 years ago. The equivalent moraines marking the southern border of the ice sheet are unknown but may be found among those extending from Lake Athabaska to southeast of Cree Lake and, farther east, among those mapped by Prest (*8*) in northwestern Ontario and eastern Manitoba. An estimate of the minimum age of the Cochrane readvance, put at 7875 ± 200 years ago [I(GSC)14] by Terasmae and Hughes (*9*), makes feasible its correlation with some part of the Cockburn system.

G. Falconer
J. T. Andrews
J. D. Ives
Geographical Branch, Canada Department of Mines and Technical Surveys, Ottawa

References and Notes

1. Geol. Assoc. Can., Glacial Map of Canada (1958).
2. W. Blake, Jr., *Can. Dept. Mines Tech. Surv. Geol. Surv. Can. Paper 63-28* (1963).
3. J. D. Ives, *Geograph. Bull. Can. No. 12* (1958); O. H. Løken, *Rept. to Arctic Inst. N. Amer.* (1964) (unpublished).
4. J. D. Ives and J. T. Andrews, *Geograph. Bull. Can. No. 19* (1963).
5. V. W. Sim, *Can. Geographer No. 17* (1960).
6. Unpublished maps prepared for Glacial Map of Canada (*1*). Glacial features were mapped from aerial photographs of northern Canada by Falconer in 1955 as part of a program supervised by J. T. Wilson, University of Toronto.
7. B. G. Craig, *Can. Dept. Mines Tech. Surv. Geol. Surv. Can. Paper 61-5* (1961); *Can. Dept. Mines Tech. Surv. Geol. Surv. Can. Geol. Surv. Bull. 99* (1964); W. Dyck and J. G. Fyles, *Radiocarbon* **4**, 24 (Yale Univ. Press, New Haven, 1962).
8. V. K. Prest, *Can. Dept. Mines Tech Surv. Geol. Surv. Can. Paper 63-6* (1963).
9. J. Terasmae and O. L. Hughes, *Science* **131**, 1444 (1960).

27 October 1964

Optical Second-Harmonic Generation in Crystalline Amino Acids

Abstract. *Optically active amino acids contain many highly efficient optical second-harmonic generators. When light from a ruby laser at 6943 Å falls on the crystalline amino acids with sufficient intensity, the second harmonic of the light at 3471 Å can be observed. Although the symmetry requirements for optical second-harmonic generation are always met by isomerically pure optically active substances, there is considerable variation in efficiency for the generation of the second harmonic, ranging from almost zero to greater than that of potassium dihydrogen phosphate, the most efficient known.*

Our earlier investigations (*1*) of two-photon absorption in organic materials showed that glass surfaces bearing finger smudges emitted ultraviolet light in the region between 3400 and 3700 Å when excited by light from a ruby laser with peak powers of the order of 100 watts. We considered the possibility that the emission might come from second-harmonic generation by amino acids whose presence in finger smudges is well known (*2*). Crystals capable of generating second harmonics of the ruby laser light must have a unit cell with no center of inversion (*3*), and this requirement is met by crystals of isomerically pure D- or L-amino acids because these molecules themselves are dissymmetric. We found that L-tryptophan as well as many other optically active amino acids are relatively efficient generators of optical second harmonics, the conversion efficiency being of the same order of magnitude as that of the best-known inorganic second-harmonic generator, potassium dihydrogen phosphate (KH_2PO_4). This behavior is almost certainly characteristic of most crystals of optically active molecular compounds of which the amino acids and peptides form a large and biologically important subclass.

It appears that the generation in the amino acids of ultraviolet-light quanta from red-light quanta may be of biologic interest. Although the conversion efficiency at light intensities ordinarily encountered in nature is extremely small, the phenomenon may provide a source of internally produced quanta of electromagnetic radiation of sufficient energy to damage nucleic acid chains; multiquantum processes such as optical harmonic generation or two-photon absorption may play some role in the generation of mutations by light of wavelengths which are normally considered biologically inactive on a one-photon basis.

The experimental arrangement used for the comparative measurements is shown schematically in Fig. 1. The laser was a Raytheon LH 5 head modified for use with an external reflecting prism and a chemical Q-switch consisting of Vd-phthalocyanine dissolved in nitrobenzene to give an optical density of approximately 0.32 at 6943 Å over a path length of 1 mm. The laser gave output pulses with a peak power of about 10 Mw and a halfwidth of 30 to 40 nsec. A Corning 2-60 glass filter in front of the laser prevented the escape of pumping light. The laser power was monitored after attenuation in 1 cm of concentrated $NiSO_4$ solution by an RCA 925 phototube operating with an anode voltage of 225 into a 50-ohm load. Laser output was focused by a lens with a focal length of 15 cm, and the samples were placed 7 cm behind this lens. Thus, the laser light focused partially on the sample into an area of roughly 0.25 cm^2. The light scattered from the sample normal to the direction of the laser beam was picked up at a distance of 25 cm, after it had passed through one 4-70 and three 7-37 Corning glass filters, by an RCA 1P28 photomultiplier operating from a 1000-volt supply and into a 50-ohm load; the filters ensured that only ultraviolet light of a narrow spectral region was picked up by the photomultiplier. Signals from the phototube and photomultiplier were displayed on the lower and upper beam of a Tektronix 555 dual-beam oscilloscope in positive and negative polarity, respectively (Fig. 2); the delay between the peaks reflected the electron transit time in the photomultiplier.

To establish that the ultraviolet signals were second harmonic and were not caused by some other luminescence of different origin, the exact wavelength and size of the bandwidth of the emitted light were determined spectroscopically (*4*) for L-tryptophan and L-leucine by means of photographic detection and also, in the case of L-tryptophan, by photoelectric detection at the output of a Beckman DU spectrophotometer converted for use as a monochromator. In both cases the linewidth was so narrow that its resolution was limited by the capability of the instrument. A very narrow linewidth at twice the laser frequency is a definite indication of harmonic generation.

Each sample was in the form of a layer of powder, 0.1 mm thick, pressed between a microscope glass slide and a cover glass. The plane of the layer was placed at an angle of 45 deg to the incident laser beam. Sample geom-

Table 1. Second-harmonic conversion efficiencies relative to potassium dihydrogen phosphate equaling 1.0.

Compound	D	L	DL
	Amino acids		
Alanine	0.40	0.20	0.40
α-Amino *n*-butyric acid	.30		
Arginine		1.50	
Asparagine HCl	.02		
Aspartic acid	.70	1.10	
Cysteine HCl	.04		
Cystine		0.02	
Ethionine	.30		
Glutamic acid	.70	.30	
Glycine			.20
Histidine HCl		.01	
Homocysteine thiolactone HCl	.20		
Isoleucine		.80	
Leucine		.90	.03
Lysine HCl		.60	
Methionine	.70	.60	.03
Phenylalanine	.15	.05	
Proline		.20	
Serine	.23	.22	.02
Tryptophan		.80	.05
Threonine	1.25	1.15	
Tyrosine	0.003	0.01	.06
Tyrosine HCl		0.02	
Valine	1.70	1.10	.01
	Sugars		
Sucrose	0.2		
Dextrose	.1		
Saccharose	.2		
D-Glucose	.1		